



This manuscript version is made available under the CC-BY-NC-ND 4.0 license  
<http://creativecommons.org/licenses/by-nc-nd/4.0/>

Shukla, B. K., et al. (2020). "A Comparison of Four Approaches to Evaluate the Sit-To-Stand Movement." IEEE Transactions on Neural Systems and Rehabilitation Engineering. Vol 28: in press.

The final version of this article is available on the publisher's website:  
<https://ieeexplore.ieee.org/document/9070208>

The DOI of the article is: <https://doi.org/10.1109/TNSRE.2020.2987357>

# A Comparison of Four Approaches to Evaluate the Sit-To-Stand Movement

Brajesh K. Shukla, Hiteshi Jain, Vivek Vijay, Sandeep K Yadav, Arvind Mathur, and David J Hewson

**Abstract**—The sit-to-stand test (STS) is a simple test of function in older people that can identify people at risk of falls. The aim of this study was to develop two novel methods of evaluating performance in the STS using a low-cost RGB camera and another an instrumented chair containing load cells in the seat of the chair to detect center of pressure movements and ground reaction forces. The two systems were compared to a Kinect and a force plate. Twenty-one younger subjects were tested when performing two 5STS movements at self-selected slow and normal speeds while 16 older fallers were tested when performing one 5STS at a self-selected pace. All methods had acceptable limits of agreement with an expert for total STS time for younger subjects and older fallers, with smaller errors observed for the chair ( $-0.18 \pm 0.17$  s) and force plate ( $-0.19 \pm 0.79$  s) than for the RGB camera ( $-0.30 \pm 0.51$  s) and the Kinect ( $-0.38 \pm 0.50$  s) for older fallers. The chair had the smallest limits of agreement compared to the expert for both younger and older participants. The new device was also able to estimate movement velocity, which could be used to estimate muscle power during the STS movement. Subsequent studies will test the device against opto-electronic systems, incorporate additional sensors, and then develop predictive equations for measures of physical function.

**Index Terms**—Biomedical monitoring, functional screening, Kinect, RGB camera, sit-to-stand.

## I. INTRODUCTION

FALLS are a major concern in older people, with around 30% of people aged over 65 falling each year, with the prevalence increasing in older age groups [1]. Risk factors for falls include low strength, poor balance and mobility problems [2]. People who are at risk of falls need to be identified to implement targeted fall-reduction programs including balance and strength training [3]. A simple test of physical function to identify fallers is the Five-times Sit-to-Stand test (5STS) [4]. The 5STS test was shown to outperform both the Timed-Up-and-Go (TUG) and single-leg stance tests in differentiating between low, moderate and high risk of falls [5]. The importance of the STS test has been highlighted in many works in the past that have used it to screen for older adults with fall risk [6, 7]. There are two main variations of the test in which the person either performs five STS as quickly as possible [8]

or the person performs as many STS as possible within 30 seconds [9].

Performance in the STS is typically measured using a stopwatch to record the time taken for the task or the number of repetitions performed. However, instrumented versions of both tests have been developed to improve the accuracy of measurement and also to extract additional information about the STS performance. Such tests have used a range of techniques including body-worn accelerometers [10, 11], pressure sensors [12], and visual sensors, often using multiple cameras [13, 14]. In addition to the possibility of automatic detection of STS time, in one study parameters extracted using a Kinect were more closely related to the strength of the participants than was the overall STS time [15]. Such a finding indicates that extracting data on the way on how the STS is performed, rather than simply the time to perform the 5STS, could be beneficial.

Previous techniques to evaluate the STS have included the use of wearable and visual sensors. For instance, a triaxial accelerometer mounted on the waist was used to classify different activities like running, walking, or postures such as sitting and lying, as well as transitional activities such as the STS and falling [10]. Accelerometers have also been used to distinguish between normal subjects and people with Parkinson's disease with respect to their STS performance as part of the TUG test [11]. Although sensor-based tests can be effective, the user is required to wear the sensors when the test is being performed, which can be inconvenient. The preferred locations of wearable sensors have been reported as the wrist, on glasses, or the arm [16]. In such cases, sensors are not good at detecting the movement of the entire body, such as that performed in the STS [17].

Other studies have used visual sensors to evaluate the STS movement. For instance, Allin et al. [14] used three cameras to extract 3-D features like the distance between the feet and head, to construct body centroids. Ellipsoid tracking was then used, along with the Weka Machine Toolkit, to classify postures based on the position of the head, feet and torso [18], with an excellent correlation observed between the Berg Balance Score and the rise time of the STS. However, this process necessitated

Submitted for review on the 8<sup>th</sup> November 2019.

B. K. Shukla is with the Indian Institute of Technology Jodhpur, Karwar 342037, India (e-mail: shukla.1@iitj.ac.in).

H. Jain is with the Indian Institute of Technology Jodhpur, Karwar 342037, India (e-mail: jain.4@iitj.ac.in).

V. Vijay is with the Indian Institute of Technology Jodhpur, Karwar 342037, India (e-mail: vivek@iitj.ac.in).

S.K. Yadav is with the Indian Institute of Technology Jodhpur, Karwar 342037, India (e-mail: sy@iitj.ac.in).

A. Mathur is with the Asian Centre for Medical Education, Research & Innovation, Jodhpur 342003, India (email: mathurarvindju@gmail.com).

D.J. Hewson is with the Institute for Health Research University of Bedfordshire, Luton LU1 3JU, UK (e-mail: david.hewson@beds.ac.uk).

manual labeling of individual body parts for one image of each subject to enable color information to be learned for each person tested. Moreover, three carefully positioned cameras were required to measure the STS time, making such a system difficult to use outside of a laboratory setting. In another study, pose-based descriptors from volumetric image data were used to identify the STS movement [19].

Activities, including the STS, were then identified and classified using the nearest neighbor method. More recently, 3-D modeling of a human body in voxel space has been used to estimate STS time [13]. This study used an ellipse-fitting algorithm that obtained features from the image to determine body orientation. The best segmentation accuracies for this method used the ellipse fit and voxel height. This framework was suggested as being suitable for real-time video monitoring of community-dwelling older people to detect fallers, with two cameras required to calculate human voxels. Furthermore, the accuracies of background subtraction are highly dependent on the type of background. A cluttered background leads to false silhouette extractions and thus a non-robust solution [20].

In response to the difficulties outlined above, the solutions developed in this paper are two-fold: 1) We propose the design of a novel device in which four force sensors are built into a chair to measure individual STS cycles, which removes the requirement for participants to wear body sensors throughout the experiment. 2) We propose a low-cost video framework to measure STS time using only a single inexpensive RGB camera. The human skeleton from the frames captured with the RGB camera is extracted using a deep learning network, with frame sequences then segmented into STS cycles using the change in the location of the head.

In this paper, we analyze the performances of these two novel approaches to evaluate the STS and compare them to two previously used instrumented systems to evaluate the STS, the Kinect, and a force plate. Our framework provides a number of advantages, such as the use of a single low-cost RGB camera that can be easily extended to android phones [15, 21, 22] and a method that does not involve background subtraction to extract the human silhouette. Although such a method has been used previously with an RGB-based camera setup [13], it fails in a cluttered environment when silhouette extraction becomes difficult. In contrast, the new method uses a deep pose library to extract body position. The use of visual sensors allows monitoring of both the time taken to perform the STS and the way it is performed, which is not possible in sensor-based approaches alone. Finally, while both STS performance and STS time can be analyzed using an RGB camera, the instrumented chair provides additional information related to the movement of the center of pressure, which could provide useful information about the STS movement.

Our goal in this study is to design a framework to evaluate the STS in an unstructured setting, without requiring human intervention. In the next section we explain the chair design and the pose estimation using the RGB camera. Next, we describe the methodology used to determine STS time and STS velocity using both the visual sensors (RGB and Kinect) and the force-based sensors (chair and force plate). We then present our

experimental results, compare the performance of the methods for the four systems, and conclude with discussions and future work.

## II. OUR FRAMEWORK

In this section we propose two new methods to estimate STS time and STS velocity during the STS movement. Firstly, an instrumented chair is designed using four load cells that eliminates the need of subjects to wear body sensors while performing the STS test. Next, we introduce a single RGB camera-based system to capture the STS movement and propose a technique to estimate STS time. A detailed description of both modules follows.

### A. Instrumented Chair Design

A wooden chair with a 47cm seat height was instrumented with four load cells, which were positioned in a cross with a distance of 31 cm between each adjacent pair of load cells. Each load cell was rated for 40 kg with a precision of 8 g (CZL 601, Standard Load Cells, Vadodara, Gujarat, India). The load cells were fixed to the seat of the chair and covered by an additional piece of wood. Each pair of load cells on one side of the chair was connected to a 24-bit analogue to digital converter (ADC) (HX711 Avia Semiconductors, Xiamen, China), with each ADC placed on a bracing strut on the side of the chair in which it was located. The two ADC receiving signals from the left and right load cells were connected to a microcontroller board (Arduino Mega 2560, Arduino LLC, Somerville, MA, USA), with data acquired at 80Hz using a custom-built software program written in Python (Fig. 1). Instantaneous center of pressure (CoP) of the forces applied through the chair was calculated as the barycenter of the four load cells signals. Anteroposterior (AP) and mediolateral (ML) displacement of the CoP were also calculated, while the sum of the forces from the individual load cells were taken to be an estimate of vertical ground reaction force ( $F_z$ ).

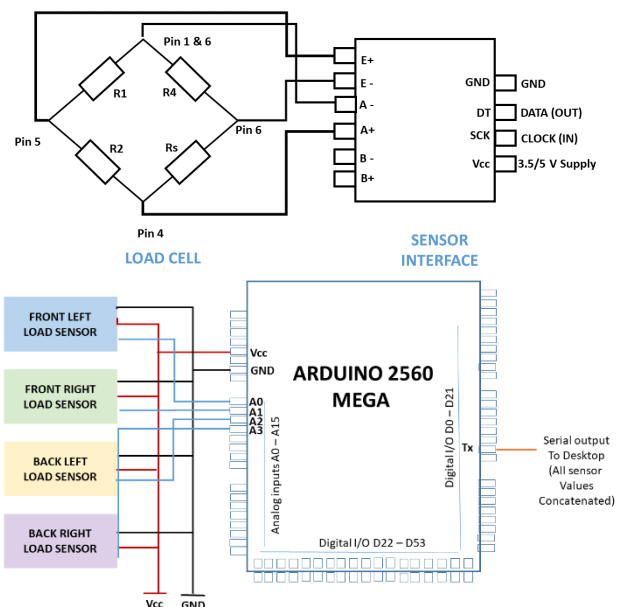


Fig. 1. Load cell – Arduino – computer Interface

It should be noted that Fz and CoP data can only be obtained when the person is in contact with the chair during the STS movement. In addition, data from the force plate is zeroed when participants are seated prior to the start of any testing. Calibration of the chair was carried out using a series of known masses, which were placed at different locations on the seat of the chair. This was used to verify the CoP and Fz data, with all values accurate to within the load cell manufacturer's specifications of  $\pm 32$  g for the mass and  $\pm 1$  mm for the CoP.

### B. Single Camera-based Posture Analysis

Cameras are readily available in the form of android devices or installed surveillance cameras. These visual sensors can be a useful resource in health care monitoring. Typically, multiple cameras are used in order to extract human silhouettes from video recordings [13, 14]. In the method developed for this study, only a novel single camera solution is used to calculate STS time.

Accurate pose estimation is essential to identify people in a video frame. This requires the location of the body to be identified in each RGB frame. One way of accomplishing this is by background subtraction and extraction of the human silhouette. Although this technique is relatively simple, it gives false boundaries when the background is cluttered, while the silhouettes do not define body joints distinctively. In contrast, the exact location of pixels that correspond to key-points of the body, also known as joint points, are required for an accurate clinical test [23].

Pose estimation is a challenge in computer vision research, with several problems arising for researchers to deal with. Any pose estimation method needs to deal with clothing, lighting conditions, background, view angles, and occlusion. With the advent of deep-learning techniques, many solutions to human pose estimation have been introduced, such as the recently-introduced Stacked Hourglass Network method [24]. Poses estimated using this library are accurate at assessing human movement [25].

The Stacked Hourglass Network method defines local features such as the wrist, ankle, elbow and the orientation and arrangement of these features with respect to each other. In order to capture the right description of human joints, the images are analyzed at different scales, with a low-level resolution for joints and a high-level resolution for orientation. The Stacked Hourglass Network consists of downscaling and upscaling layers, which resembles an hourglass that is stacked multiple times. The result of this deep network model is a set of K heatmaps that correspond to K joint points. The network is pre-trained on two datasets FLIC and MPII such that it can easily predict different orientations of human bodies.

A pose consisting of 15 joint locations was estimated by the network for each frame of the image, as shown in Fig. 2. The joint locations used are head, right and left shoulder, right and left elbow, right and left wrist, pelvis, right and left hip, right and left knee, and right and left ankle. A sample estimation for a subject performing the STS is shown in Fig. 3, with the skeleton on the left and heat maps of joint estimation probability on the right.

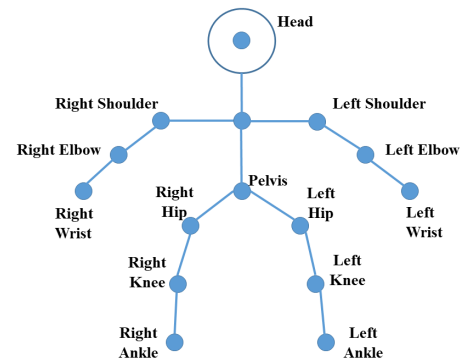


Fig. 2. The 15-segment model of a pose used to estimate the STS

Calibration of the camera was performed using the chair as a reference, with the back of the chair measuring 0.5m. This was used to ensure that the pixels within the image that covered the chair corresponded to 0.5m when the other measurements were taken. For all recordings, the camera was placed 2.3 m on a line perpendicular to the front of the chair. The frame of reference used for the 3D data from Kinect has the IR sensor as the origin, while the RGB camera, which is in 2D, has the origin at the top left corner of the image. The frame of reference for both sensors transformed a frame of reference fixed on the body of the subject, with nearest hip of the subject taken as the origin in all directions of movement.

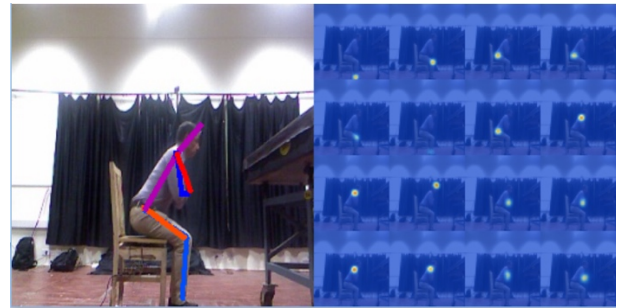


Fig. 3. Example of pose estimation during the STS movement

### C. STS Parameter Calculation

The total time taken for each 5STS was estimated for each of the four recording systems. The method used to estimate STS time for both the RGB and Kinect systems was adapted from that of Ejupi et al. [15]. This consists of an estimation of the head position obtained from the camera for the duration of the recording. Position data were low pass filtered with a 4th order Butterworth filter with a 2Hz cut-off frequency. The peaks identified were taken to be the mid-point of the standing positions while the troughs were taken to be the mid-point of the sitting positions. If the head position was within 5cm of the nearest peak the subject was considered to be standing, while a position within 5cm of the nearest valley was taken to be sitting. An example of head position signals during the 5STS for the RGB and Kinect systems is shown in Fig. 4(a-b).

The mean duration of the 5STS was calculated for the force plate and the chair, as shown in Fig. 4(c-d). Force data were also low pass filtered with a 4th order Butterworth filter with a 2Hz cut-off frequency. For the force plate, the start of each sit-to-

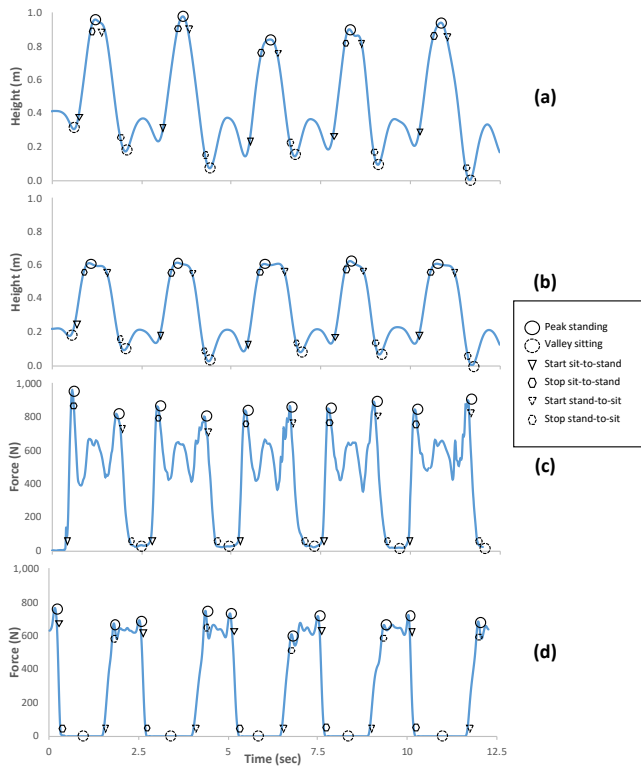


Fig. 4. Calculation of STS time and STS phases for RGB camera (a), Kinect (b), force plate (c) and chair (d).

stand phase was taken to be 10% of the peak force obtained during the transition to a standing position, which corresponds to the same ratio as the 5cm value used for the two camera-based systems when compared to the mean standing height of 50 cm. A subject was considered to be standing when the force reached 90% of the peak force for the individual STS. The standing phase of the STS was considered to have finished when vertical force decreased below 90% of peak force, with subjects considered to have returned to a sitting position when vertical force reached 10% of the previous peak. For the chair, the opposite method was used since force decreases during the sit-to-stand but increases for the force plate. Accordingly, for the chair sit-to-stand phase, when vertical force decreased below 90% of peak force, subjects were considered to have started to stand up, while a subject was considered to be standing when their force decreased below 10% of peak. The same approach was used for the stand-to-sit, which began when force reached 10% of peak force, with subjects considered to be sitting when 90% of peak force was reached.

In addition to total STS time, a worthwhile parameter that can be obtained from an instrumented STS is sit-to-stand velocity. STS velocity is better able to distinguish between fallers and non-fallers, than total STS time [15]. STS velocity was calculated for the two camera-based systems using the method proposed by Ejupi et al. [15] for the period between the end of the sitting phase and the standing phase of each STS movement. The height change between these two points was divided by the time taken to obtain STS velocity. For the force plate and the chair, velocity was derived using Newton's second law of motion between the time when force was between 10%

and 90% of maximal force during the sit-to-stand movement. The force-time curve was divided by mass to produce an acceleration-time curve, which was then numerically integrated using the trapezoid rule to produce the velocity-time curve from which peak STS velocity was obtained. The average of STS velocity for the five STS movements was used in all subsequent analyses.

#### D. Comparison of STS Parameters

The performance of the four systems was compared using data collected from a sample of 21 healthy younger subjects and a sample of 16 older fallers. The younger participants performed two trials, the first of which was at a self-selected slow speed, while subjects were asked to perform the second trial as fast as possible. The older fallers performed a single trial at a self-selected speed. The ethics committee of the Asian Centre for Medical Education, Research & Innovation approved the study (ACMERI/18/001), with all subjects giving informed consent.

Comparative performances of the four methods of obtaining STS time and STS velocity were undertaken using correlation analysis and limits of agreement, using Bland-Altman plots [26]. Overall STS time was compared to a reference time that was obtained from the analysis of a frame-by-frame record of each STS from the RGB camera [13]. The expert manually identified the beginning and end of each STS, with the beginning taken to be when the subject began to move their torso forward in the first STS, while the end of the STS was estimated as the moment when the subject's torso returned to vertical after completing the 5th STS movement. These start and endpoints were chosen based on the four phases of the STS movement described previously [27]. The use of an expert assessment of the video as the gold-standard for STS time was chosen rather than a stopwatch, as previous research has reported errors due to delays in starting the stopwatch after the command was given to start being included in the time, while errors also occur when stopping the timer [13].

All four methods were compared with that of the expert for total 5STS time using Bland-Altman plots. For STS velocity, no expert velocity was available, therefore Bland-Altman plots were not used. All data processing was performed using custom-built software developed using LabVIEW (Version 2018, National Instruments Corporation, Austin, Texas, USA). Statistical analysis was performed using SPSS (version 25, IBM Corporation, Armonk, New York, USA).

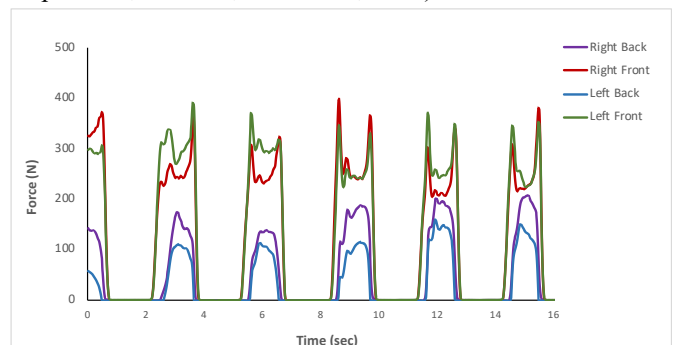


Fig. 5. Example recording from the instrumented chair during the 5STS test

### III. RESULTS

The young subjects were aged  $28.3 \pm 6.8$  years, weighed  $67.2 \pm 9.6$  kg, of height  $1.70 \pm 0.04$  m, with BMI  $23.2 \pm 3.0$  kg/m<sup>2</sup>, while the fallers were aged  $67.2 \pm 6.7$  years, weighed  $64.3 \pm 12.0$  kg, of height  $1.58 \pm 0.07$  m, with BMI  $25.9 \pm 4.2$  kg/m<sup>2</sup>. The time for the slow 5STS was  $13.0 \pm 1.9$  s, as timed by the expert. The time for the fast 5STS was  $10.3 \pm 1.4$  s, while the fallers performed the 5STS in  $18.0 \pm 3.4$  s. A typical example recording from the instrumented chair is shown in Fig. 5.

TABLE I  
PERFORMANCE OF THE TESTING SYSTEMS FOR 5STS TIME FOR YOUNG

	Kinect	RGB	Force plate	Chair
Time (s)	$10.8 \pm 1.9$	$10.6 \pm 1.9$	$11.7 \pm 2.2$	$11.8 \pm 2.2$
Correlation	0.990*	0.997*	0.979*	0.995*
95% CI	0.975 - 0.996	0.993 - 0.998	0.948 - 0.991	0.988 - 0.998
Error (s)	$-0.84 \pm 0.35$	$-1.01 \pm 0.23$	$-0.05 \pm 0.33$	$-0.16 \pm 0.17$
LOA (s)	1.38	0.91	1.31	0.67
LOA (%)	90.9%	95.5%	97.7%	97.7%

Times and mean errors are means  $\pm$  SD; limits of agreement are range and percentage of points within this range. LOA: Limits of Agreement. \*Correlation is significantly different from zero ( $p < 0.05$ ).

TABLE II  
PERFORMANCE OF THE TESTING SYSTEMS FOR 5STS TIME FOR FALLERS

	Kinect	RGB	Force plate	Chair
Time (s)	$17.6 \pm 3.3$	$17.7 \pm 3.6$	$17.8 \pm 3.5$	$17.7 \pm 3.1$
Correlation	0.979*	0.983*	0.948*	0.988*
95% CI	0.939 - 0.992	0.951 - 0.994	0.854 - 0.982	0.965 - 0.996
Error (s)	$-0.38 \pm 0.50$	$-0.30 \pm 0.51$	$-0.19 \pm 0.79$	$-0.18 \pm 0.17$
LOA (s)	1.97	1.98	3.08	0.67
LOA (%)	93.8%	93.8%	100%	100%

Times and mean errors are means  $\pm$  SD; limits of agreement are range and percentage of points within this range. LOA: Limits of Agreement. \*Correlation is significantly different from zero ( $p < 0.05$ ).

#### A. Total STS Time

The performances of the four systems for young subjects for 5STS time against the expert time of  $11.7 \pm 2.1$  s are shown in Table 1. The performance for 5STS time for the older fallers compared to the expert time of  $18.0 \pm 3.4$  s is shown in Table 2. Bland Altman plots of the limits of agreement for the four methods for both groups of subjects combined when compared to the expert values are shown in Fig. 6.

When the ranking of each system was compared for the four measures of performance used against the expert, the chair had the best performance. For the older fallers, the chair had the highest correlation, smallest error, the narrowest range for the limits of agreement, and the highest percentage of points within this range. When the younger subjects were considered, the chair was the best for both LOA measures, along with two-second rankings for the correlation and error measures.

#### B. STS Velocity

Comparisons for STS velocity are shown in Table 3 for younger participants and in Table 4 for the older fallers. The two camera-based systems obtained higher velocities than the two force-based systems. When the younger and older faller results were

TABLE III  
PERFORMANCE OF THE TESTING SYSTEMS FOR STS VELOCITY FOR YOUNG

	Kinect	RGB	Force plate	Chair
Velocity (m/s)	$0.94 \pm 0.16$	$0.93 \pm 0.17$	$0.89 \pm 0.20$	$0.74 \pm 0.20$
Correlation	0.811*		0.905*	
95% CI	(0.678 - 0.892)		(0.832 - 0.947)	
Mean diff. (s)	$-0.02 \pm 0.16$		$-0.16 \pm 0.09$	

Times and mean differences are means  $\pm$  SD. \*Correlation is significantly different from zero ( $p < 0.05$ ).

TABLE IV  
PERFORMANCE OF THE TESTING SYSTEMS FOR STS VELOCITY FOR FALLERS

	Kinect	RGB	Force plate	Chair
Velocity (m/s)	$0.59 \pm 0.12$	$0.64 \pm 0.37$	$0.65 \pm 0.18$	$0.53 \pm 0.15$
Correlation	0.574*		0.796*	
95% CI	(0.109 - 0.833)		(0.496 - 0.926)	
Mean diff. (s)	$-0.05 \pm 0.35$		$-0.12 \pm 0.11$	

Times and mean differences are means  $\pm$  SD. \*Correlation is significantly different from zero ( $p < 0.05$ ).

compared, greater discrepancies for a given system were observed for the two camera-based systems than for the two force-based systems, with lower correlations and higher mean differences, especially for the fallers. A comparison of the STS velocity measures from the four devices was made with gait velocity for the group of older fallers. The highest correlation with gait velocity was obtained for chair STS velocity ( $r=0.76$ ), followed by the force plate ( $r=0.49$ ), RGB camera ( $r=0.12$ ), and the Kinect ( $r=0.07$ ).

### IV. DISCUSSION

In this study, two new methods were proposed to evaluate the STS movement, which is an important functional screening tool in older people. One method used pose estimation from a single RGB camera, while the other method used an instrumented chair. The findings showed that both methods performed as well or better than previously reported methods in which a Kinect and a force plate were used to calculate total STS time and STS velocity, both of which can differentiate between fallers and non-fallers.

Both new methods had an excellent agreement with an expert estimation of STS in terms of the number of data points that fell within 2SD of the mean difference. However, the camera method underestimated the total STS time compared to the expert by around one second. In contrast, the chair method had an average error within 0.2 sec of the expert time. This suggests that the newly developed chair can accurately detect STS time and could offer an alternative to a manual method. The reason for the differences is most likely due to the difficulty in using head height to detect the start of the STS, which begins with a forward movement of the trunk before the second phase of vertical movement occurs [27]. To improve the accuracy of the camera-based techniques, it might be necessary to include the detection of forwards movement, rather than the vertical movement described previously [15].

In addition to detecting overall STS time, it would be



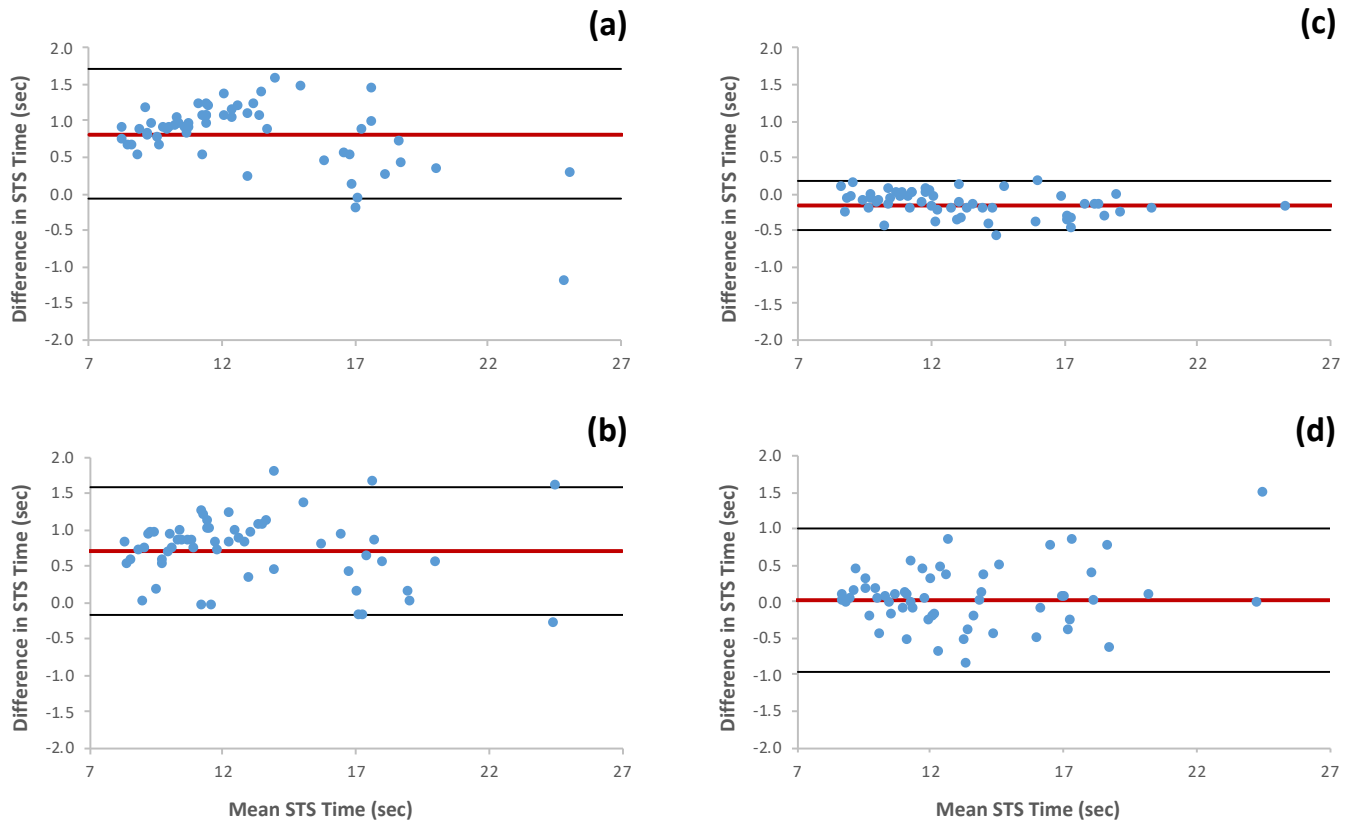


Fig. 6. Limits of agreement between expert STS time and the four systems; (a) RGB Camera; (b) Kinect; (c) Force plate; (d) Chair

worthwhile identifying the time spent in each STS to detect fatigue as the STS is performed. Previous work has associated fatigue with increasingly slower times for the individual STS measured by the use of force plates and IMU [28]. This could offer an additional advantage when compared to a standard stopwatch method typically used in clinical settings. The error of the chair method was less than 10% of the minimal detectable change for the 5STS, which has been reported to be 2.5 seconds [29]. Previous work has shown that instrumented versions of the 5STS typically obtain quicker times than those when using a stopwatch [15, 30].

The different methods were also compared for the STS velocity parameter. In this case, it wasn't possible to use an expert for comparative purposes as it isn't possible to calculate velocity from a non-instrumented STS test. When the methods were compared for younger subjects, similar values for STS velocity were observed for all systems. Likewise, when the older fallers were considered, similar values were also observed across the systems. For all of the systems, lower STS velocities were observed for the older fallers, as would be expected. When the estimates of STS velocity for the devices were compared with gait velocity, the two force-based measures performed far better than those based on visual analysis. A high correlation was found with gait velocity for the chair, with a moderate correlation for the force plate.

There appears to be two possibilities for the lower correlations for the camera-based systems with gait velocity. Firstly, the accuracy of the methods themselves used to determine the head height from which velocity was estimated could have been inaccurate, which would have resulted in the

differences observed. This could be further investigated using an optoelectronic system to record human movement, such as the Vicon, which would also confirm the accuracy of all systems presented in this work and act as a gold standard. Secondly, using head height to determine STS velocity could be the issue. During the STS there is a transition phase when sitting, with hip flexion occurring as the subject bends forwards before standing up. This can be seen in Fig 4. for both camera-based systems, with height decreasing before standing up. This could create variability in the camera-based systems, meaning that the force-based measures might be superior, although a larger study is needed to confirm this finding.

The results of this study show that the chair could be used to evaluate the STS in clinical settings, providing a potentially cheaper alternative than a force plate. The total cost of the components in the chair was approximately \$100, which although not the commercial cost of a final product, would be substantially cheaper than a standard force plate, which typically cost thousands of dollars. In addition, when detecting STS time it was also possible to estimate STS velocity, which has been shown to distinguish between older controls and those with a history of hip fracture [31]. It would also be possible to estimate the power produced during the STS using the method proposed by Lindemann et al., in which the difference between seated height and standing height is combined with the rate of force development to estimate power [32]. Power during the STS is a strong predictor of overall muscle power and even cross-sectional area of the quadriceps [33, 34], which means the instrumented chair might be able to estimate muscle mass.

This study is not without limitations. Firstly, the system has

thus far only been tested on young healthy subjects and one cohort of older fallers so needs to be validated on a wider range of older participants to determine the predictive ability of the system in terms of other conditions associated with aging, such as frailty and sarcopenia. Also, the present chair design does not enable all of the individual phases of the STS to be detected, particularly when the user is no longer in contact with the chair. The absence of a gold standard against which to compare STS velocity obtained from the four systems is also a limitation. Although the observed relationship between STS velocity and gait velocity was encouraging, it would have been useful to have measures of leg strength for the older subjects rather than using gait velocity as a proxy measure. Finally, the analysis performed was not automated, which would make the tests more widely applicable in clinical settings.

The limitations in terms of STS phase detection will be addressed in future work using infrared sensors to detect body position and joint angles, such as hip flexion. Future work could also examine whether fusion of both chair and RGB systems would be of benefit. Finally, it would be worth evaluating whether the system could predict muscle power and/or muscle mass, as has been demonstrated by previous work with the STS test [33, 34].

## V. CONCLUSION

This paper presented the development of two novel systems to evaluate the STS movement. The instrumented chair performed the best at detecting the STS when compared to an expert, with encouraging results also obtained when STS velocity was compared to physical function. Future work will use additional sensors to estimate muscle power during the STS.

## REFERENCES

- [1] C. R. Gale, C. Cooper, and A. A. Sayer, "Prevalence and risk factors for falls in older men and women: The English Longitudinal Study of Ageing," *Age Ageing*, vol. 45, no. 6, pp. 789-794, 2016, doi: 10.1093/ageing/afw129.
- [2] T. Masud and R. O. Morris, "Epidemiology of falls," *Age Ageing*, vol. 30, no. suppl 4, pp. 3-7, 2001, doi: 10.1093/ageing/30.suppl\_4.3.
- [3] C. A. Pfortmueller, G. Lindner, and A. K. Exadaktylos, "Reducing fall risk in the elderly: risk factors and fall prevention, a systematic review," *Minerva Med*, vol. 105, no. 4, pp. 275-281, 2014.
- [4] R. W. Bohannon, "Sit-to-Stand Test for Measuring Performance of Lower Extremity Muscles," *Percept Mot Skills*, vol. 80, no. 1, pp. 163-166, 1995, doi: 10.2466/pms.1995.80.1.163.
- [5] S. Buatois *et al.*, "Five times sit to stand test is a predictor of recurrent falls in healthy community-living subjects aged 65 and older," *J Am Geriatr Soc*, vol. 56, no. 8, pp. 1575-1577, 2008, doi: 10.1111/j.1532-5415.2008.01777.x.
- [6] A. Kerr, D. Rafferty, K. M. Kerr, and B. Durward, "Timing phases of the sit-to-walk movement: Validity of a clinical test," *Gait Posture*, vol. 26, no. 1, pp. 11-16, 2007, doi: 10.1016/j.gaitpost.2006.07.004.
- [7] A. Tiedemann, H. Shimada, C. Sherrington, S. Murray, and S. Lord, "The comparative ability of eight functional mobility tests for predicting falls in community-dwelling older people," *Age Ageing*, vol. 37, no. 4, pp. 430-435, 2008, doi: 10.1093/ageing/afn100.
- [8] S. L. Whitney, D. M. Wrisley, G. F. Marchetti, M. A. Gee, M. S. Redfern, and J. M. Furman, "Clinical Measurement of Sit-to-Stand Performance in People With Balance Disorders: Validity of Data for the Five-Times-Sit-to-Stand Test," *Phys Ther*, vol. 85, no. 10, pp. 1034-1045, 2005.
- [9] C. J. Jones, R. E. Rikli, and W. C. Beam, "A 30-s chair-stand test as a measure of lower body strength in community-residing older adults," *Res Q Exerc Sport*, vol. 70, no. 2, pp. 113-119, 1999, doi: 10.1080/02701367.1999.10608028.
- [10] D. W. Kang, J. S. Choi, J. W. Lee, S. C. Chung, S. J. Park, and G. R. Tack, "Real-time elderly activity monitoring system based on a tri-axial accelerometer," *Disabil Rehabil Assist Technol*, vol. 5, no. 4, pp. 247-53, 2010, doi: 10.3109/17483101003718112.
- [11] A. Weiss *et al.*, "Can an accelerometer enhance the utility of the Timed Up & Go Test when evaluating patients with Parkinson's disease?," *Med Eng Phys*, vol. 32, no. 2, pp. 119-125, 2010, doi: 10.1016/j.medengphy.2009.10.015.
- [12] A. Arcelus, I. Veledar, R. Goubran, F. Knoefel, H. Sveistrup, and M. Bilodeau, "Measurements of Sit-to-Stand Timing and Symmetry From Bed Pressure Sensors," *IEEE Trans Instrum Meas*, vol. 60, no. 5, pp. 1732-1740, May 2011, doi: 10.1109/tim.2010.2089171.
- [13] T. Banerjee, M. Skubic, J. M. Keller, and C. Abbott, "Sit-to-Stand Measurement for In-Home Monitoring Using Voxel Analysis," *IEEE J Biomed Health Inform*, vol. 18, pp. 1502-1509, 2014, doi: 10.1109/JBHI.2013.2284404.
- [14] S. Allin and A. Mihailidis, "Low-cost, Automated Assessment of Sit-To-Stand Movement in "Natural" Environments," in *4th European Conference of the International Federation for Medical and Biological Engineering*, Berlin, Heidelberg, 2009, vol. 22: Springer, in IFBME Proceedings, pp. 76-79, doi: 10.1007/978-3-540-89208-3\_20.
- [15] A. Ejupi, M. Brodie, Y. J. Gschwind, S. R. Lord, W. L. Zagler, and K. Delbaere, "Kinect-based five-times-sit-to-stand test for clinical and in-home assessment of fall risk in older people," *Gerontology*, vol. 61, no. 1, pp. 118-124, 2016, doi: 10.1159/000381804.
- [16] J. Cho, "Current Status and Prospects of Health-Related Sensing Technology in Wearable Devices," *J Healthc Eng*, vol. 2019, Art no. 3924508, doi: 10.1155/2019/3924508.
- [17] H. Matsuyama, K. Hiroi, K. Kaji, T. Yonezawa, and N. Kawaguchi, "Hybrid Activity Recognition for Ballroom Dance Exercise using Video and Wearable Sensor," in *2019 Joint 8th International Conference on Informatics, Electronics & Vision (ICIEV) and 2019 3rd International Conference on Imaging, Vision & Pattern Recognition (icIVPR)*, 30 May-2 June 2019 2019, pp. 112-117, doi: 10.1109/ICIEV.2019.8858524.
- [18] I. H. Witten, E. Frank, M. A. Hall, and C. J. Pal, *Data Mining: Practical machine learning tools and techniques*, 4th ed. Cambridge, MA, USA: Morgan Kaufmann, 2016.
- [19] S. Pehlivan and P. Duygulu, "A new pose-based representation for recognizing actions from multiple cameras," *Comput Vis Image Underst*, vol. 115, no. 2, pp. 140-151, 2011, doi: 10.1016/j.cviu.2010.11.004.
- [20] J. K. Aggarwal and Q. Cai, "Human motion analysis: A review," *Comput Vis Image Underst*, vol. 73, no. 3, pp. 428-440, 1999, doi: 10.1006/cviu.1998.0744.
- [21] H. Pirsiavash, C. Vondrick, and A. Torralba, "Assessing the Quality of Actions," in *European Conference on Computer Vision*, Zurich, 2014: Springer International Publishing, in Computer Vision – ECCV 2014, pp. 556-571, doi: doi.org/10.1007/978-3-319-10599-4\_36.
- [22] H. Jain and G. Harit, "A framework to assess sun salutation videos," in *Proceedings of the Tenth Indian Conference on Computer Vision, Graphics and Image Processing*, Guwahati, Assam, India, 18-22 December, 2016 2016: Association for Computing Machinery, pp. 29:1-29:8, doi: doi.org/10.1145/3009977.3010045.
- [23] K. Chen *et al.*, "Patient-Specific Pose Estimation in Clinical Environments," *IEEE J Transl Eng Health Med*, vol. 6, pp. 1-11, 2018, doi: 10.1109/JTEHM.2018.2875464.
- [24] A. Newell, K. Yang, and J. Deng, "Stacked Hourglass Networks for Human Pose Estimation," in *European Conference on Computer Vision*, Amsterdam, 2016: Springer International Publishing, in Computer Vision – ECCV 2016, pp. 483-499, doi: 10.1007/978-3-319-46484-8\_29.
- [25] H. Jain and G. Harit, "Detecting missed and anomalous action segments using approximate string matching algorithm," in *Computer Vision, Pattern Recognition, Image Processing, and Graphics: 6th National Conference, NCVPRIPG 2017*, Mandi, India, 2018: Springer, pp. 101-111.



- [26] J. M. Bland and D. G. Altman, "Measuring agreement in method comparison studies," *Stat Methods Med Res*, vol. 8, no. 2, pp. 135-60, 1999.
- [27] P. J. Millington, B. M. Myklebust, and G. M. Shambes, "Biomechanical analysis of the sit-to-stand motion in elderly persons," *Arch Phys Med Rehabil*, vol. 73, no. 7, pp. 609-617, 1992, doi: 10.5555/uri:pii:000399939290124F.
- [28] S. Hellmers *et al.*, "Measurement of the Chair Rise Performance of Older People Based on Force Plates and IMUs," *Sensors*, vol. 19, no. 6, p. 1370, 2019, doi: doi.org/10.3390/s19061370.
- [29] A. Goldberg, M. Chavis, J. Watkins, and T. Wilson, "The five-times-sit-to-stand test: validity, reliability and detectable change in older females," *Aging Clin Exp Res*, vol. 24, no. 4, pp. 339-344, 2012, doi: 10.1007/bf03325265.
- [30] K. Kaewkaen, S. Uttama, W. Rueangsirarak, and P. Kaewkaen, "Test-retest Reliability of the Five Times Sit-to-Stand Test measured using the kinect in older adults," *Journal of Associated Medical Sciences*, vol. 52, pp. 138-144, 05/01 2019.
- [31] J. Houck, J. Kneiss, S. V. Bukata, and J. E. Puzas, "Analysis of vertical ground reaction force variables during a Sit to Stand task in participants recovering from a hip fracture," *Clin Biomech*, vol. 26, no. 5, pp. 470-476, 2011, doi: 10.1016/j.clinbiomech.2010.12.004.
- [32] U. Lindemann, R. Muehe, M. Stuber, W. Zijlstra, K. Hauer, and C. Becker, "Coordination of strength exertion during the chair-rise movement in very old people," *J Gerontol A Biol Sci Med Sci*, vol. 62, no. 6, pp. 636-640, 2007, doi: 10.1093/gerona/62.6.636.
- [33] W. N. Smith *et al.*, "Simple equations to predict concentric lower-body muscle power in older adults using the 30-second chair-rise test: a pilot study," *Clin Interv Aging*, vol. 5, pp. 173-180, 2010, doi: doi.org/10.2147/cia.s7978.
- [34] Y. Takai, M. Ohta, R. Akagi, H. Kanehisa, Y. Kawakami, and T. Fukunaga, "Sit-to-stand test to evaluate knee extensor muscle size and strength in the elderly: a novel approach," *J Physiol Anthropol*, vol. 28, no. 3, pp. 123-128, 2009, doi: 10.2114/jpa2.28.123.